

Errata, Clarifications, & Additional Material

December 14, 2024

For *Applied Numerical Methods for Partial Differential Equations* by Carl L. Gardner, Springer, 2024

Errata

Clarifications

p 130, 2nd paragraph: Requiring $\Delta t \leq h/c$ for stability is [an example of](#) the CFL condition: ...

p 132, 2nd paragraph: *FTCS* for $u_t + cu_x = 0$ satisfies the CFL condition [for \$r \leq 1\$](#) but is unconditionally unstable: ...

Add after sentence with (8.149) on p 160: [In \(8.149\), the forward-in-time \$\Delta w/\Delta t\$ is a shorthand for any consistent and stable \(explicit\) timestepping scheme like RK3.](#)

p 169, 3rd paragraph: ...two copies of the 1D code ([see \(8.149\)](#)), one for the x sweep for evaluating $f(w)_x$ and one for the y sweep for evaluating $g(w)_y$.

p 172, 3rd paragraph: ...two copies of the 1D WENO3 method ([see \(8.149\)](#)): [an \$x\$ sweep for calculating \$f\(w\)_x\$ and a \$y\$ sweep for calculating \$g\(w\)_y\$.](#)

p 192 after (9.40): ... $\Delta \mathbf{u}/\Delta t$ is a shorthand for any consistent [and stable](#) (explicit) timestepping scheme ...

Additional Material

Space-Time Stencils for Classical Parabolic Methods

The stencils for classical methods for time-dependent PDEs are shown in Figs. 1–8. In these diagrams, space is horizontal and time is vertical. Figure 3 is annotated to indicate spatial grid points $i - 1$, i , and $i + 1$ and time levels n and $n + 1$. To compute the new solution u_i^{n+1} with the trapezoidal rule method, for example, the old solution values u_i^n and $u_{i\pm 1}^n$ are coupled with the new solution values u_i^{n+1} and $u_{i\pm 1}^{n+1}$.

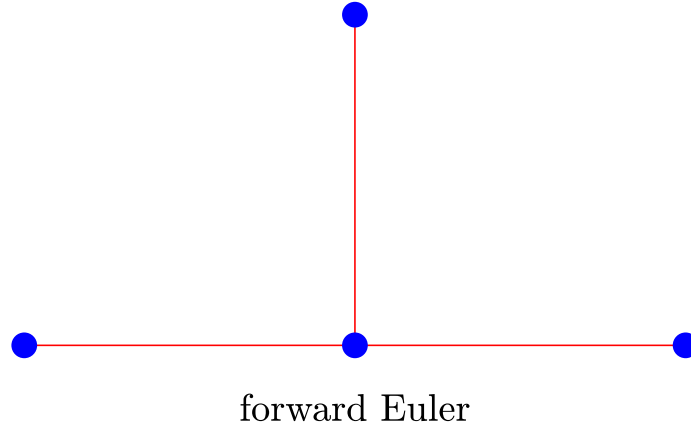


Figure 1: Space-time stencil for the forward Euler parabolic method.

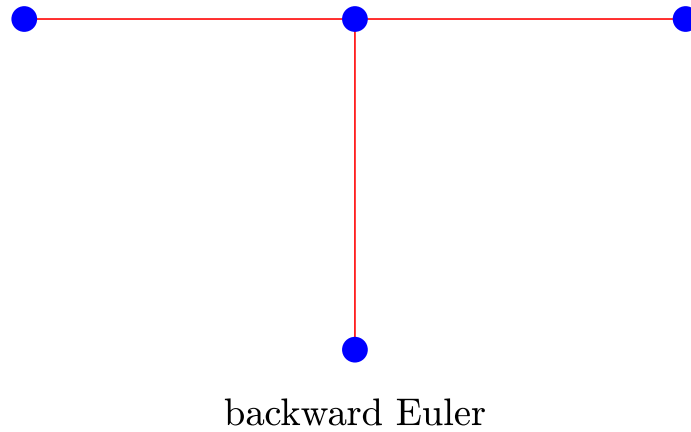


Figure 2: Space-time stencil for the backward Euler parabolic method.

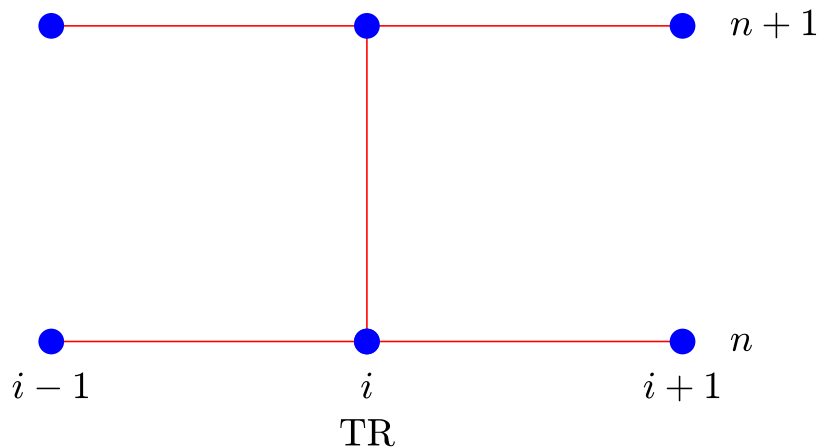


Figure 3: Annotated space-time stencil for the trapezoidal rule parabolic method.

Space-Time Stencils for Classical Hyperbolic Methods

Figures 4–8 display the stencils for the classical hyperbolic methods, where again space is horizontal and time is vertical. The cyan line is the characteristic for $u_t + cu_x = 0$ flowing into the new solution point u_i^{n+1} . For stability, the characteristic must lie within the domain of dependence of the discrete scheme (by virtue of the CFL condition), which implies $c\Delta t \leq \Delta x$ (see Figs. 4 and 5). The CFL condition is necessary but not sufficient for stability: the FTCS method in Fig. 7 satisfies the CFL condition for $\Delta t \leq \Delta x/c$, but is always unstable for hyperbolic PDEs.

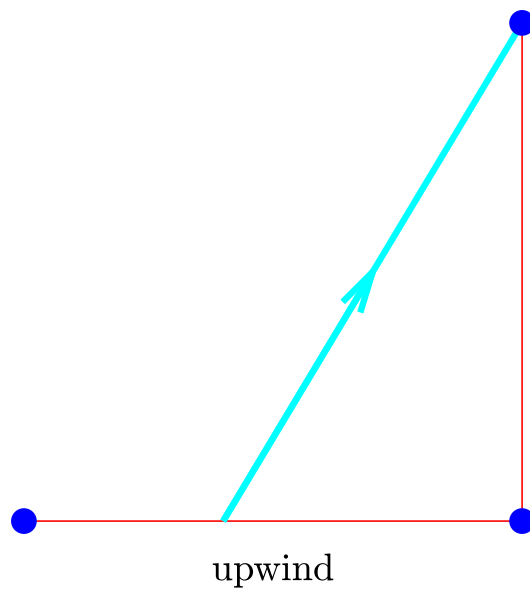


Figure 4: Stable space-time stencil for the upwind hyperbolic method for $u_t + cu_x = 0$ with $c\Delta t < \Delta x$. The foot of the characteristic lies inside the domain of dependence of the difference scheme, satisfying the CFL condition.

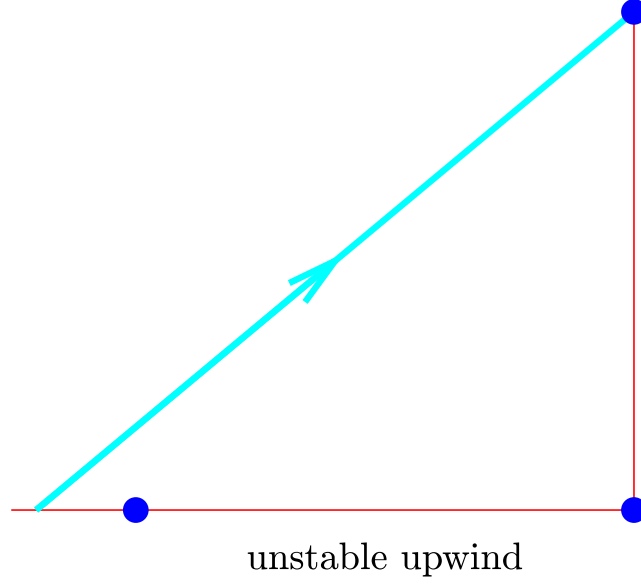


Figure 5: Unstable space-time stencil for the upwind hyperbolic method for $u_t + cu_x = 0$ with $c\Delta t > \Delta x$. The foot of the characteristic now lies outside the domain of dependence of the difference scheme, violating the CFL condition.

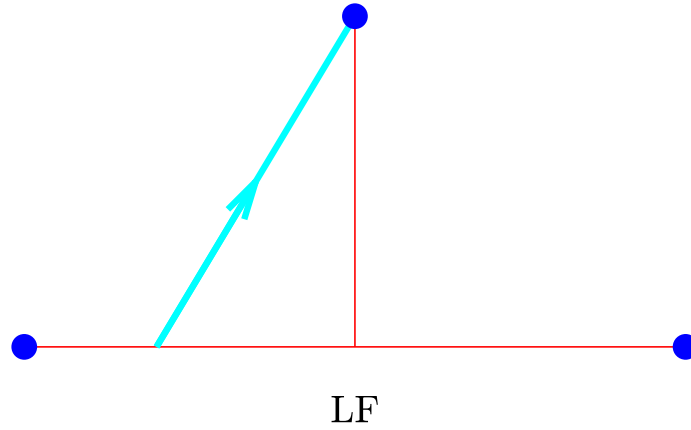


Figure 6: Space-time stencil for the Lax-Friedrichs hyperbolic method for $u_t + cu_x = 0$ with $c\Delta t < \Delta x$.

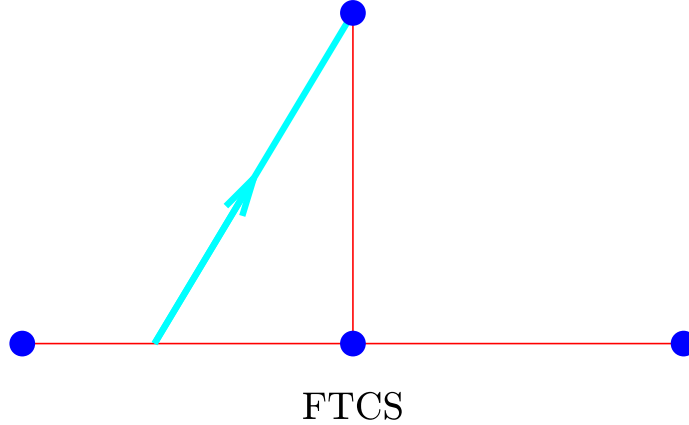


Figure 7: Space-time stencil for the *always unstable* forward time central space method when applied to hyperbolic PDEs.

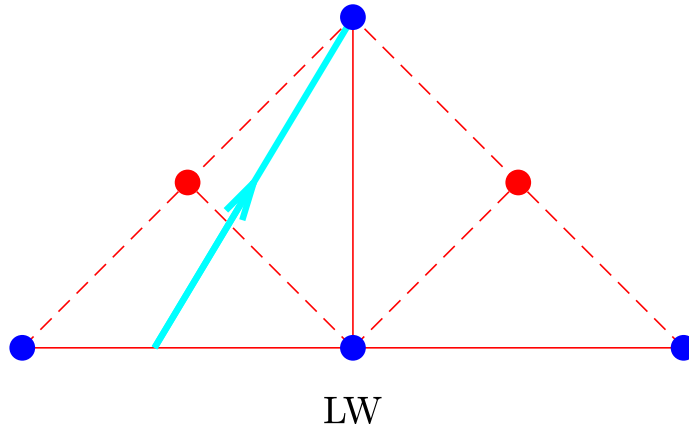


Figure 8: Space-time stencil for the Lax-Wendroff hyperbolic method for $u_t + cu_x = 0$ with $c\Delta t < \Delta x$. The red dots are at time level $n + \frac{1}{2}$ and grid points $i \pm \frac{1}{2}$.